GEOPHYSICS, VOL. 73, NO. 6 (NOVEMBER-DECEMBER 2008); P. F247–F259, 7 FIGS., 7 TABLES.
10.1190/1.2976115

A comparison between Gauss-Newton and Markov-chain Monte Carlo–based methods for inverting spectral induced-polarization data for Cole-Cole parameters

Jinsong Chen[1], Andreas Kemna[2], and Susan S. Hubbard[1]

ABSTRACT

We have developed a Bayesian model to invert spectral induced-polarization (SIP) data for Cole-Cole parameters using Markov-chain Monte Carlo (MCMC) sampling methods. We compared the performance of the MCMC-based stochastic method with an iterative Gauss-Newton-based deterministic method for Cole-Cole parameter estimation through inversion of synthetic and laboratory SIP data. The Gauss-Newton-based method can provide an optimal solution for given objective functions under constraints, but the obtained optimal solution generally depends on the choice of initial values and the estimated uncertainty information often is inaccurate or insufficient. In contrast, the MCMC-based inversion method provides extensive global information on unknown parameters, such as the marginal probability distribution functions, from which we can obtain better estimates and tighter uncertainty bounds of the parameters than with the deterministic method. In addition, the results obtained with the MCMC method are independent of the choice of initial values. Because the MCMC-based method does not explicitly offer a single optimal solution for given objective functions, the deterministic and stochastic methods can complement each other. For example, the stochastic method can be used first to obtain the medians of unknown parameters by starting from an arbitrary set of initial values. The deterministic method then can be initiated using the medians as starting values to obtain the optimal estimates of the Cole-Cole parameters.

INTRODUCTION

The induced-polarization (IP) method has been used increasingly in environmental investigations because IP measurements are very sensitive to the low frequency capacitive properties of rocks and soils. These properties are associated with diffusion-controlled polarization processes that occur at the mineral-fluid interface (Slater and Lesmes, 2002). The Cole-Cole model (Cole and Cole, 1941) has been very useful for interpreting spectral IP (SIP) data in terms of parameters, such as chargeability and time constant, which are used to estimate various subsurface properties (Lesmes and Friedman, 2005). Among many studies in which Cole-Cole parameters are estimated from SIP measurements on soils and rocks, the majority use classical deterministic inversion methods, specifically the iterative Gauss-Newton-based schemes with the Levenberg-Marquardt damping for stabilization of the inverse solution (Pelton et al., 1984; Jaggar and Fell, 1988; Luo and Zhang, 1998; Kemna, 2000; Boadu and Seabrook, 2000).

Two popular routines have been developed for Cole-Cole parameter estimation according to iterative Gauss-Newton algorithms. The first, developed by Pelton et al. (1978), has been demonstrated extensively on SIP data from mineralized rock; the second, developed by Kemna (2000), has been used widely for inverting SIP data associated with sediments and calibrated materials (Kemna et al., 2000, 2005; Binley et al., 2005; Slater et al., 2005, 2006; Mansoor and Slater, 2007). Although the two routines differ in terms of parameterization and definition of data, they commonly use derivatives of the forward model with respect to model parameters (i.e., Jacobian matrix) to iteratively update the Cole-Cole parameters from a set of initial values.

The main limitation of the Gauss-Newton-based deterministic method is that convergence to the global minimum is not guaranteed,

Manuscript received by the Editor 19 November 2007; revised manuscript received 5 June 2008; published online 14 November 2008; corrected version published online 19 November 2008.
[1]Lawrence Berkeley National Laboratory, Earth Sciences Division, Berkeley, California, U.S.A. Email: jchen@lbl.gov; sshubbard@lbl.gov.
[2]Formerly Agrosphere (ICG-4), Forschungszentrum Jülich, Germany; presently University of Bonn, Department of Geodynamics and Geophysics, Bonn, Germany. Email: kemna@geo.uni-bonn.de.

and estimation results strongly depend on the choice of starting values. Consequently, successful application of the deterministic method for SIP data inversion requires considerable familiarity with characteristics of Cole-Cole model responses and with sensitivity to the underlying Cole-Cole parameters. A multiple Cole-Cole model typically is used for describing SIP responses when multiple relaxation mechanisms are superimposed. In such cases, it often is difficult to choose suitable sets of initial values to obtain an optimal solution of the Cole-Cole parameters.

Other types of inversion approaches have been suggested to reduce the dependence of the optimal solution on initial values. Examples include a direct scheme by Xiang et al. (2001), which consists of a multifold least-squares estimation combined with an optimal searching technique, a genetic algorithm by Cao et al. (2005), and a robust Gauss-Newton-based method with adaptive regularization by Roy (1999). The main disadvantage of these methods is that they provide inaccurate or insufficient information on uncertainty in the parameter estimation.

Ghorbani et al. (2007) develop a Bayesian model to invert time- and frequency-domain IP data for parameters in a single Cole-Cole model. They use a numerical integration technique over regular grids to obtain a marginal posterior probability density function (pdf) of each Cole-Cole parameter from the joint posterior probability distribution function. Through case studies based on synthetic and laboratory data sets, they demonstrate that the Bayesian model could provide the estimates of the marginal probability density function of each unknown parameter and of each pair of unknown parameters. However, their method for obtaining many samples from the joint posterior distribution is very difficult to apply in practice because of the high dimensionality of the unknown parameter space, which commonly occurs with a multiple Cole-Cole model. As described in the next section, a multiple Cole-Cole model is a more general and proper model than a single Cole-Cole model for describing IP data with various dispersion ranges, caused either by multiple-length scales in sediments or by coupling effects in the IP measurements.

We begin with a review of the Cole-Cole model. This is followed by development of a Bayesian model to invert SIP data for Cole-Cole parameters using Markov-chain Monte Carlo (MCMC) sampling methods (Gilks et al., 1996). MCMC methods are effective for drawing samples from complex and high-dimensional joint probability distribution functions; they have been used increasingly to invert complex geophysical data (Bosch, 1999; Buland and Omre, 2003; Gunning and Glinsky, 2004; Chen et al., 2004, 2006). Our goal is to develop an inversion approach that is insensitive to initial values and that provides sufficient uncertainty information on the estimation when we invert SIP data for parameters in a multiple Cole-Cole model. We evaluate the performance of the sampling-based Bayesian model by applying it to synthetic and laboratory SIP data sets and comparing the inversion results with those obtained from the Gauss-Newton-based deterministic method developed by Kemna (2000).

COLE-COLE MODEL

We interpret spectral induced polarization data using the Cole-Cole model (Cole and Cole, 1941; Pelton et al., 1978), which is an empirical extension of the classic Debye relaxation model. For complex resistivity, describing the electric-voltage response to an electric-current excitation in the frequency domain, the Cole-Cole model can be written as

$$\rho(\omega) = \rho_0\left\{1 - m\left[1 - \frac{1}{1 + (j\omega\tau)^c}\right]\right\}, \qquad (1)$$

where ρ_0 is the asymptotic resistivity value toward zero frequency, m is the chargeability that describes the magnitude of electric polarization giving rise to the phase shift between voltage and current (i.e., the complex nature of ρ), τ is the characteristic time constant of the relaxation process, and c is the Cole-Cole exponent that describes the degree of frequency dependence of ρ.

In the equation, ω and j are the angular frequency and $\sqrt{-1}$, respectively. For $c = 1$, the Cole-Cole model is reduced to the Debye model. Table 1 lists variables and symbols used in this paper. Note that both Cole-Cole and Debye models are characterized by a single peak in the complex resistivity phase spectrum; the location of the peak along the frequency axis is related directly to the relaxation time constant τ.

Pelton et al. (1978) introduced the Cole-Cole model to describe electrical properties in mineralized rock, in which polarization occurs at interfaces between electronically conducting mineral grains and fluid-filled pores with electrolytic conduction. Over the last decade, the model has been adopted to describe the observed complex resistivity response of sedimentary rock that does not include electronically conducting components (Vanhala, 1997; Binley et al., 2005; Kemna et al.,

Table 1. Nomenclature.

Symbol	Meaning
ρ, ρ^{obs}	Complex resistivity
ω, ω_k	Angular frequency
f_k	Frequency
ρ_0, $\rho_0^{(0)}$, $\rho_0^{(t)}$	Zero-frequency resistivity
m, m_l, m_1, m_2, m_L	Chargeability
τ, τ_l, τ_1, τ_2, τ_L	Time constant
c, c_l, c_1, c_2, c_L	Cole-Cole exponent
u_{Re}, $u_{\text{Re}}^{(0)}$, $u_{\text{Re}}^{(t-1)}$, $u_{\text{Re}}^{(t)}$	Inverse variance of errors in real part of data
u_{Im}, $u_{\text{Im}}^{(0)}$, $u_{\text{Im}}^{(t-1)}$, $u_{\text{Im}}^{(t)}$	Inverse variance of errors in imaginary part of data
Re[ ], Im[ ]	Real and imaginary part of complex resistivity
$\mathbf{m}$, $\mathbf{m}^{(0)}$, $\mathbf{m}^{(t-1)}$, $\mathbf{m}^{(t)}$	Base 10 logarithmic chargeability vector
$\mathbf{b}$, $\mathbf{b}^{(0)}$, $\mathbf{b}^{(t-1)}$, $\mathbf{b}^{(t)}$	Base 10 logarithmic time-constant vector
$\mathbf{c}$, $\mathbf{c}^{(0)}$, $\mathbf{c}^{(t-1)}$, $\mathbf{c}^{(t)}$	Dependence-factor vector
e_k^r	Relative error
$N(\mu_\rho^*, u_\rho^*)$	Normal distribution with mean μ_ρ^* and inverse variance u_ρ^*
Ind( )	Indicator function
$\Gamma(\alpha,\lambda)$	Gamma distribution with shape parameter α and inverse scale parameter λ

2005) and that normally exhibits a much weaker phase response than does mineralized rock. In that case, polarization is a result of the interaction of the pore fluid (electrolyte) with electrically charged mineral surfaces, on which the so-called electric double layer is formed (e.g., Leroy et al., 2008).

Importantly for both polarization mechanisms, the observed time scale of relaxation, as quantified by the Cole-Cole time constant τ, is related directly to the length scale determined by the size of electronically conducting grains in mineralized rock (Pelton et al., 1978) or by the length scale characteristic of the pore space in sedimentary rock (e.g., Titov et al., 2002; Scott and Barker, 2003; Binley et al., 2005; Slater, 2007). In this sense, the measured complex resistivity spectrum represents an integrated response over all length scales presented in the rock (e.g., Leroy et al., 2008). For rock with a unimodal distribution of length scales (i.e., a unimodal grain or pore-size distribution), a phase spectrum with a single peak, as reported repeatedly in the literature, can be expected. However, for more complex distributions of length scales such as bimodal distributions, phase spectra with more than one phase peak can be observed (Leroy et al., 2008). The different peaks reflect relaxation processes at different scales. Such behavior also is observed in time-domain measurements of induced polarization (Tong et al., 2006; Tarasov and Titov, 2007).

An additional frequency dependence in the measured complex resistivity spectrum typically is generated by inductive and/or capacitive coupling effects associated with instrumentation and cable layout. These coupling effects can be described phenomenologically also by a Cole-Cole dispersion term (e.g., Pelton et al., 1978; Kemna et al., 1999, 2005). In this case, however, the Cole-Cole parameters themselves normally are not of interest, but only the response of the parameter set with an objective of removing it from the measured data.

We adopt a multiple Cole-Cole model as used by Kemna (2000) to allow for analysis of phase spectra with more than one dispersion range caused either by the multiple modality of the rock or by coupling effects in the measurements. Such a model represents a discrete integration over different relaxation scales and is given by

$$\rho(\omega) = \rho_0\left\{1 - \sum_{l=1}^{L} m_l\left[1 - \frac{1}{1 + (j\omega\tau_l)^{c_l}}\right]\right\}, \quad (2)$$

where L is the number of Cole-Cole models that we fit for a given complex resistivity data set. A typical value for L is between 1 and 3, depending on the number of present relaxation scales and whether the inversion procedure is applied to remove coupling effects from the measured data or to extract intrinsic Cole-Cole parameters from complex resistivity imaging results (Kemna et al., 2000). The symbols m_l, τ_l, and c_l represent chargeability, time constant, and dependence factor for the lth dispersion term in the multiple Cole-Cole model, respectively.

The Cole-Cole model given in equation 2 can be rewritten in the form of real and imaginary components of complex resistivity as given by Cao et al. (2005),

$$\mathrm{Re}[\rho(\omega_k)] = \rho_0\left[1 - \sum_{l=1}^{L} m_l\left(1 - \frac{R_l}{R_l^2 + I_l^2}\right)\right], \quad (3)$$

and

$$\mathrm{Im}[\rho(\omega_k)] = -\rho_0\sum_{l=1}^{L} m_l\frac{I_l}{R_l^2 + I_l^2}, \quad (4)$$

where $\omega_k = 2\pi f_k, k = 1,2,\ldots,n$ (f_k is the kth frequency, and n is the total number of frequencies at which the IP measurements are collected), $R_l = (\omega_k\tau_l)^{c_l}\cos(c_l\pi/2) + 1$, and $I_l = (\omega_k\tau_l)^{c_l}\sin(c_l\pi/2)$.

STOCHASTIC METHOD

Bayesian framework

We develop a Bayesian model to estimate parameters in the Cole-Cole model given by equations 3 and 4. The SIP data used for this model are the real and imaginary components (i.e., $\mathrm{Re}[\rho^{\mathrm{obs}}(\omega_k)]$ and $\mathrm{Im}[\rho^{\mathrm{obs}}(\omega_k)]$) of the complex resistivity collected at frequency ω_k ($k = 1,2,\ldots,n$). The unknown parameters are the zero-frequency resistivity ρ_0, the base 10 logarithmic chargeability $\mathbf{m} = (\log(m_1), \log(m_2),\ldots,\log(m_L))^T$, the base 10 logarithmic time constant $\mathbf{b} = (\log(\tau_1),\log(\tau_2),\ldots,\log(\tau_L))^T$, and the dependence factor $\mathbf{c} = (c_1,c_2,\ldots,c_L)^T$. To account for unknown measurement errors in the real and imaginary components, we include two additional parameters u_{Re} and u_{Im}, which are the inverse variances of measurement errors in the real and imaginary parts of complex resistivity.

As a result, we can write the Bayesian model as

$$\begin{aligned} f(\rho_0,\mathbf{m},\mathbf{b},\mathbf{c},u_{\mathrm{Re}},u_{\mathrm{Im}}|\{&\mathrm{Re}[\rho^{\mathrm{obs}}(\omega_k)],\mathrm{Im}[\rho^{\mathrm{obs}}(\omega_k)],\\ &k = 1,2,\ldots,n\}) \\ &\propto \prod_{k=1}^{n} f(\mathrm{Re}[\rho^{\mathrm{obs}}(\omega_k)]|\rho_0,\mathbf{m},\mathbf{b},\mathbf{c},u_{\mathrm{Re}}) \\ &\quad\times \prod_{i=1}^{n} f(\mathrm{Im}[\rho^{\mathrm{obs}}(\omega_k)]|\rho_0,\mathbf{m},\mathbf{b},\mathbf{c},u_{\mathrm{Im}}) \\ &\quad\times f(\rho_0,\mathbf{m},\mathbf{b},\mathbf{c},u_{\mathrm{Re}},u_{\mathrm{Im}}). \end{aligned} \quad (5)$$

The first and second terms on the right side of equation 5 are likelihood functions of the real and imaginary components of complex resistivity data, respectively; the third term is the prior distribution function of unknown Cole-Cole parameters. Because we assume that errors in the real and imaginary parts of complex resistivity at different frequencies are independent of each other, we can write the expression in the form of the product of individual likelihood functions as shown in equation 5. Below, we define the likelihood functions and prior distributions that are included in the equation.

Likelihood functions

To define the likelihood function of the real components of complex resistivity, we assume that relative errors between the observed data and the output of the forward Cole-Cole model have a normal distribution with zero mean and unknown inverse variance, that is,

$$e_k^r = \frac{\mathrm{Re}[\rho^{\mathrm{obs}}(\omega_k)] - \mathrm{Re}[\rho(\omega_k)]}{\mathrm{Re}[\rho^{\mathrm{obs}}(\omega_k)]} \sim N(0,u_{\mathrm{Re}}). \quad (6)$$

We choose this likelihood model partly because errors in IP data often have a distribution close to the normal distribution, and partly because the maximum likelihood estimates of such types of likelihood

functions are equal to the estimates of the deterministic method (i.e., the least-squares estimation).

With this error distribution, the likelihood function of the real components is given by

$$f(\mathrm{Re}[\rho^{\mathrm{obs}}(\omega_k)]|\rho_0,\mathbf{m},\mathbf{b},\mathbf{c},u_{\mathrm{Re}}) = \sqrt{\frac{u_{\mathrm{Re}}}{2\pi}}\exp\left(-\frac{u_{\mathrm{Re}}}{2}\left(\frac{\mathrm{Re}[\rho^{\mathrm{obs}}(\omega_k)]-\mathrm{Re}[\rho(\omega_k)]}{\mathrm{Re}[\rho^{\mathrm{obs}}(\omega_k)]}\right)^2\right). \quad (7)$$

Similarly, we can define the likelihood function of the imaginary components of complex resistivity as

$$f(\mathrm{Im}[\rho^{\mathrm{obs}}(\omega_k)]|\rho_0,\mathbf{m},\mathbf{b},\mathbf{c},u_{\mathrm{Im}}) = \sqrt{\frac{u_{\mathrm{Im}}}{2\pi}}\exp\left(-\frac{u_{\mathrm{Im}}}{2}\left(\frac{\mathrm{Im}[\rho^{\mathrm{obs}}(\omega_k)]-\mathrm{Im}[\rho(\omega_k)]}{\mathrm{Im}[\rho^{\mathrm{obs}}(\omega_k)]}\right)^2\right). \quad (8)$$

Prior models

The prior distribution of Cole-Cole parameters is determined from prior knowledge or other information about the parameters, which might be subjective and site-specific. Because we assume that each parameter is independent of others, we can write the joint prior distribution given in equation 5 as the product of prior distributions of each individual parameter,

$$f(\rho_0,\mathbf{m},\mathbf{b},\mathbf{c},u_{\mathrm{Re}},u_{\mathrm{Im}}) = f(\rho_0)f(\mathbf{m})f(\mathbf{b})f(\mathbf{c})f(u_{\mathrm{Re}})f(u_{\mathrm{Im}}). \quad (9)$$

To minimize subjectivity, we assume in this study that the parameters ρ_0, $\mathbf{m}$, $\mathbf{b}$, and $\mathbf{c}$ have uniform distributions over given ranges. For example, for synthetic case studies presented in the section of synthetic studies, the prior ranges of parameters ρ_0, $\mathbf{m}$, $\mathbf{b}$, and $\mathbf{c}$ are given as (1, 1000) (in Ωm), (−5,0), (−5,5) (log τ, τ in s), and (0, 1), respectively.

We similarly use proper noninformative prior distributions for inverse variances u_{Re} and u_{Im} as done in the software of the Bayesian inference using Gibbs sampling (BUGS) (Spiegelhalter et al., 1994), which are the gamma distribution with shape and inverse scale parameters of 1e-3. The above prior models are quite noninformative. As a result, the estimates of Cole-Cole parameters obtained from the stochastic method primarily depend on the data and thus are comparable to those obtained from the Gauss-Newton-based deterministic method.

SAMPLING METHODS

We obtain estimates of unknown parameters by drawing many samples from the joint posterior pdf defined in equation 5 using MCMC methods. MCMC methods provide a powerful approach for sampling multivariate variables from a complex joint probability distribution. They are superior over conventional Monte Carlo methods because the conventional methods draw independent samples and are prohibitive for drawing samples from high-dimensional joint distribution functions. As opposed to deterministic methods, which seek a single optimal solution of unknown parameters, MCMC sampling-based stochastic methods draw many samples from the joint posterior pdf. The obtained samples then can be used to infer statistics of each parameter, such as its mean, variance, and predictive intervals. As described in the following subsections, we use different methods to draw samples from the joint posterior distribution for Cole-Cole parameters, for zero-frequency resistivity, and for inverse variances of data.

Conditional probability distributions of Cole-Cole model parameters

We first derive the conditional pdfs of Cole-Cole parameters $\mathbf{m}$, $\mathbf{b}$, and $\mathbf{c}$. Because the conditional distribution of each of those parameters is similar, we describe only the method for obtaining the conditional distribution of chargeability vector $\mathbf{m}$, given all other unknown parameters and SIP data. Because MCMC sampling methods concern only the quantities that are functions of vector $\mathbf{m}$, we can obtain the conditional $f(\mathbf{m}|\cdot)$ by keeping those terms that are related to vector $\mathbf{m}$. The result is given by

$$f(\mathbf{m}|\cdot) \propto \mathrm{Ind}(\mathbf{m}\in D_{\mathbf{m}})\prod_{k=1}^{n} f(\mathrm{Re}[\rho^{\mathrm{obs}}(\omega_k)]| \rho_0,\mathbf{m},\mathbf{b},\mathbf{c},u_{\mathrm{Re}})\prod_{k=1}^{n} f(\mathrm{Im}[\rho^{\mathrm{obs}}(\omega_k)]|\rho_0,\mathbf{m},\mathbf{b},\mathbf{c},u_{\mathrm{Im}}). \quad (10)$$

The first term on the right side of equation 10 is an indicator variable that accounts for the constraint from the prior distribution of vector $\mathbf{m}$, where $D_{\mathbf{m}}$ is the given prior range of chargeability. Similarly, we can obtain conditional pdfs of Cole-Cole parameters $\mathbf{b}$ and $\mathbf{c}$.

Conditional probability distribution of zero-frequency resistivity

We can obtain the analytical form of the conditional pdf of the zero-frequency resistivity because the real and imaginary components of SIP data are linear functions of it. We simplify equations 3 and 4 as $\mathrm{Re}[\rho(\omega_k)] = \rho_0 A(\omega_k)$ and $\mathrm{Im}[\rho(\omega_k)] = \rho_0 B(\omega_k)$ by letting

$$A(\omega_k) = 1 - \sum_{l=1}^{L} m_l\left(1-\frac{R_l}{R_l^2+I_l^2}\right)$$

and

$$B(\omega_k) = -\sum_{l=1}^{L} m_l\frac{I_l}{R_l^2+I_l^2}$$

Consequently, the conditional pdf has a truncated normal distribution (see Appendix A),

$$f(\rho_0|\cdot) \propto \mathrm{Ind}(\rho_0\in D_\rho)N(\mu_\rho^*,u_\rho^*), \quad (11)$$

where D_ρ is the given prior range of zero-frequency resistivity;

$$u_\rho^* = u_{\mathrm{Re}}\sum_{k=1}^{n}\left(\frac{A(\omega_k)}{\mathrm{Re}[\rho^{\mathrm{obs}}(\omega_k)]}\right)^2 + u_{\mathrm{Im}}\sum_{k=1}^{n}\left(\frac{B(\omega_k)}{\mathrm{Im}[\rho^{\mathrm{obs}}(\omega_k)]}\right)^2,$$

and

$$\mu_\rho^* = \left(u_{\mathrm{Re}}\sum_{k=1}^{n}\frac{A(\omega_k)}{\mathrm{Re}[\rho^{\mathrm{obs}}(\omega_k)]} + u_{\mathrm{Im}}\sum_{k=1}^{n}\frac{B(\omega_k)}{\mathrm{Im}[\rho^{\mathrm{obs}}(\omega_k)]}\right)\frac{1}{u_\rho^*}.$$

Conditional probability distributions of the inverse variances of measurement errors

Because prior distributions of the inverse variances of measurement errors are conjugate priors for the likelihood models defined in equations 7 and 8, we also can obtain the analytic forms of their conditional distributions, which are gamma distributions (see Appendix B), as follows,

$$f(u_{\mathrm{Re}}|\cdot) \propto f(u_{\mathrm{Re}}) \prod_{k=1}^{n} f(\mathrm{Re}[\rho^{\mathrm{obs}}(\omega_k)]|\rho_0,\mathbf{m},\mathbf{b},\mathbf{c},u_{\mathrm{Re}})$$

$$\propto \Gamma(\alpha + 0.5n, \lambda + 0.5S_{\mathrm{Re}}), \tag{12}$$

and

$$f(u_{\mathrm{Im}}|\cdot) \propto f(u_{\mathrm{Im}}) \prod_{k=1}^{n} f(\mathrm{Im}[\rho^{\mathrm{obs}}(\omega_k)]|\rho_0,\mathbf{m},\mathbf{b},\mathbf{c},u_{\mathrm{Im}})$$

$$\propto \Gamma(\alpha + 0.5n, \lambda + 0.5S_{\mathrm{Im}}), \tag{13}$$

where $\alpha = \lambda = 1e-3$,

$$S_{\mathrm{Re}} = \sum_{k=1}^{n} \left(\frac{\mathrm{Re}[\rho^{\mathrm{obs}}(\omega_k)] - \mathrm{Re}[\rho(\omega_k)]}{\mathrm{Re}[\rho^{\mathrm{obs}}(\omega_k)]} \right)^2,$$

and

$$S_{\mathrm{Im}} = \sum_{k=1}^{n} \left(\frac{\mathrm{Im}[\rho^{\mathrm{obs}}(\omega_k)] - \mathrm{Im}[\rho(\omega_k)]}{\mathrm{Im}[\rho^{\mathrm{obs}}(\omega_k)]} \right)^2.$$

Sampling algorithm and monitoring convergence

We use the Gibbs sampler (Geman and Geman, 1984) to draw samples from the joint posterior distribution defined in equation 5. The main steps are listed below:

1) Assign initial values to ρ_0, $\mathbf{m}$, $\mathbf{b}$, $\mathbf{c}$, u_{Re}, and u_{Im}; refer to them as $\rho_0^{(0)}$, $\mathbf{m}^{(0)}$, $\mathbf{b}^{(0)}$, $\mathbf{c}^{(0)}$, $u_{\mathrm{Re}}^{(0)}$, and $u_{\mathrm{Im}}^{(0)}$, respectively. Let $t = 1$.
2) Draw a sample from $f(\rho_0|\cdot)$ given $\mathbf{m}^{(t-1)}$, $\mathbf{b}^{(t-1)}$, $\mathbf{c}^{(t-1)}$, $u_{\mathrm{Re}}^{(t-1)}$, and $u_{\mathrm{Im}}^{(t-1)}$; refer to it as $\rho_0^{(t)}$.
3) Draw a sample from $f(\mathbf{m}|\cdot)$ given $\rho_0^{(t)}$, $\mathbf{b}^{(t-1)}$, $\mathbf{c}^{(t-1)}$, $u_{\mathrm{Re}}^{(t-1)}$, and $u_{\mathrm{Im}}^{(t-1)}$; refer to it as $\mathbf{m}^{(t)}$.
4) Draw a sample from $f(\mathbf{b}|\cdot)$ given $\rho_0^{(t)}$, $\mathbf{m}^{(t)}$, $\mathbf{c}^{(t-1)}$, $u_{\mathrm{Re}}^{(t-1)}$, and $u_{\mathrm{Im}}^{(t-1)}$; refer to it as $\mathbf{b}^{(t)}$.
5) Draw a sample from $f(\mathbf{c}|\cdot)$ given $\rho_0^{(t)}$, $\mathbf{m}^{(t)}$, $\mathbf{b}^{(t)}$, $u_{\mathrm{Re}}^{(t-1)}$, and $u_{\mathrm{Im}}^{(t-1)}$; refer to it as $\mathbf{c}^{(t)}$.
6) Draw a sample from $f(u_{\mathrm{Re}}|\cdot)$ given $\rho_0^{(t)}$, $\mathbf{m}^{(t)}$, $\mathbf{b}^{(t)}$, $\mathbf{c}^{(t)}$, and $u_{\mathrm{Im}}^{(t-1)}$; refer to it as $u_{\mathrm{Re}}^{(t)}$.
7) Draw a sample from $f(u_{\mathrm{Im}}|\cdot)$ given $\rho_0^{(t)}$, $\mathbf{m}^{(t)}$, $\mathbf{b}^{(t)}$, $\mathbf{c}^{(t)}$, and $u_{\mathrm{Re}}^{(t)}$; refer to it as $u_{\mathrm{Im}}^{(t)}$.
8) Let $t = t + 1$. If $t > T$, where T is the maximum number of iterations allowed, stop; otherwise, go to step 2.

We can obtain many samples of unknown Cole-Cole parameters and inverse variances of measurement errors, i.e., $\{\rho_0^{(t)}, \mathbf{m}^{(t)}, \mathbf{b}^{(t)}, \mathbf{c}^{(t)}, u_{\mathrm{Re}}^{(t)}, u_{\mathrm{Im}}^{(t)}, t = 1,2,\ldots,T\}$, by following the aforementioned algorithm. Theoretically, after a sufficiently long run (e.g., t_0 iterations, referred to as burn-in by Gilks et al., 1996), the drawn samples are approximately the samples drawn from the true joint pdf given in equation 5. Many methods can be used to find the burn-in number and to monitor the convergence of the obtained Markov chains, such as the methods developed by Gelman and Rubin (1992), Geweke (1992), and Raftery and Lewis (1992); we use the Gelman and Rubin (1992) method in this study.

We run three chains by starting from different sets of initial values for the total number of T iterations. As the samples drawn early in the process could depend on the starting values, we throw away the first $0.5T$ number of samples for each chain and consider them as the burn-in. We calculate a criterion, referred to as the scale reduction score in Gelman and Rubin (1992), based on the three Markov chains. With that approach, if the scale reduction score is less than 1.2, the Markov chain is considered to be converged; otherwise, more runs are needed.

SYNTHETIC STUDIES

We first demonstrate the use of the sampling-based Bayesian model for Cole-Cole parameter estimation using a synthetic SIP data set. We then compare the results obtained from the stochastic approach with those obtained from the deterministic method developed by Kemna (2000). We choose a synthetic case with a dual Cole-Cole model because this case often is encountered in practice, either to describe an SIP response with two relaxation domains or to describe a single-relaxation SIP response contaminated by capacitive

Table 2. True Cole-Cole parameters of the synthetic dual model, the prior ranges and initial values of the stochastic method, and the initial values of the deterministic method for inverting the synthetic SIP data.

Cole-Cole parameters	True values	Stochastic inversion				Deterministic inversion initial values (Init0)
		Prior ranges	Initial-1	Initial-2	Initial-3	
ρ_0 (Ωm)	25.00	(1,1000)	5.0	50.0	500.0	20.0
m_1	0.50	(1e − 5,1)	0.1	0.4	0.6	0.1
$\log(\tau_1)$ (τ_1 in s)	1.00	(−5,5)	−4.0	−1.0	1.0	1.0
c_1	0.40	(0,1)	0.1	0.4	0.6	0.5
m_2	0.01	(1e − 5,1)	0.1	0.4	0.6	0.1
$\log(\tau_2)$ (τ_2 in s)	0.00	(−5,5)	−4.0	−1.0	1.0	−1.0
c_2	0.98	(0,1)	0.1	0.4	0.6	0.5

and/or inductive coupling associated with the measurement layout (Pelton et al., 1978; Kemna et al., 1999).

True Cole-Cole model parameters and synthetic IP data

The synthetic Cole-Cole model parameters are listed in the second column of Table 2. These values are the same as those used by Cao et al. (2005), except for the zero-frequency resistivity whose value was not provided. The dual Cole-Cole model is separated mainly by the two chargeabilities, which have a ratio of 50. We generated synthetic SIP data using frequencies ranging from 1 mHz through 10 kHz as is typical of SIP measurements, and added 1% relative random noise to the real and imaginary components of the generated resistivity data. This level of noise is reasonable based on the noise distributions estimated from the laboratory SIP data presented in the section of laboratory studies.

Inversion procedure of the MCMC-based stochastic method

We start to invert the SIP data using common and wide (i.e., non-informative) prior ranges, specifically (1, 1000) (in Ωm) for the zero-frequency resistivity ρ_0, (1e-5, 1) for chargeabilities m_1 and m_2, (0, 1) for dependence factors c_1 and c_2, and $(-5,5)$ (in seconds) for base 10 logarithmic time constants $\log(\tau_1)$ and $\log(\tau_2)$ (see column 3 of Table 2). We run three Markov chains using three sets of initial values given by the fourth, fifth, and sixth columns of Table 2. We run each chain by beginning with one of the three sets of initial values for 20,000 iterations and use the latter half to estimate the marginal posterior pdf of each Cole-Cole parameter. The CPU time for the sampling is on the order of minutes using a personal computer with 1.8 GHz speed.

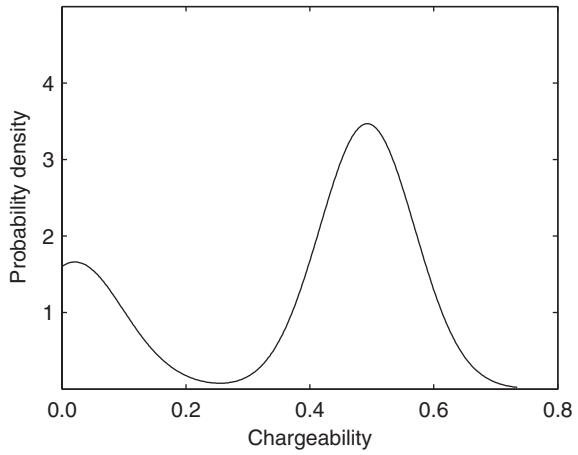

Figure 1. Estimated chargeability (m_1) for synthetic dual Cole-Cole model data using the common prior ranges.

Figure 1 shows the estimated marginal pdf of chargeability m_1, obtained stochastically using the synthetic SIP data with 1% relative noise. Two modes appear in the pdf: One is close to 0.0 and the other is about 0.5. This is because if we switch the values between the Cole-Cole parameters (m_1,τ_1,c_1) and (m_2,τ_2,c_2), the IP responses calculated from equations 3 and 4 do not change. To avoid the bimodality, we rerun the Markov chains by modifying the prior ranges of chargeability as follows, (0.25, 1) for m_1 and (1e-5, 0.25) for m_2. Using such a two-step procedure, we obtain the marginal posterior pdfs of all Cole-Cole parameters with a unique mode.

Comparison between the stochastic and deterministic inversion methods

In this subsection, we explore how the choice of initial values impacts the deterministic and stochastic estimation results, and we assess the uncertainty information provided by these inversion methods.

Dependence on the choice of initial values

The choice of initial values is not critical for the stochastic inversion method because it affects only the speed of convergence of Markov chains to the target probability distribution being sampled, but not the inversion results. In fact, it is essential for the MCMC-based methods to run multiple chains with very different sets of initial values to avoid possible local convergence. Although the stochastic method provides extensive information about each unknown parameter, we use only the medians as the best estimates and compare them with the estimates obtained from the deterministic method. In the third column of Table 3, we show the estimated medians of unknown Cole-Cole parameters based on all three Markov chains obtained using the three initial sets given in Table 2, because the estimated medians from each chain are almost identical. From the comparison be-

Table 3. Comparison of estimates from inversion of the SIP data with 1% relative noise using stochastic and deterministic methods.

			Deterministic inversion		
Cole-Cole parameters	True values	Stochastic inversion medians	Estimates (using Init0)	Estimates (using true values)	Estimates (using medians)
ρ_0 (Ωm)	25.00	25.01	24.92	25.01	25.02
m_1	0.50	0.496	0.410	0.490	0.490
$\log(\tau_1)$ (τ_1 in s)	1.00	1.009	0.878	1.009	1.012
c_1	0.40	0.398	0.416	0.398	0.397
m_2	0.01	0.015	0.100	0.016	0.017
$\log(\tau_2)$ (τ_2 in s)	0.00	0.147	1.218	0.137	0.145
c_2	0.98	0.836	0.311	0.896	0.881

tween the estimated medians and their corresponding true values, which are given in the second column of Table 3, we can see that even if we start from very different initial values, the MCMC-based method can provide good estimates of unknown parameters.

The choice of initial values is critical for the deterministic inversion, especially when considering a multiple Cole-Cole model. We found that the method often cannot converge given an arbitrary choice of initial values. For example, when we applied the initial values given in Table 2 for the stochastic inversion to the deterministic inversion method, none could converge to a solution that was close to the true values. A main problem caused by the dependence of estimates on initial values is that if differences between resultant data misfits for estimates obtained from different sets of initial values are subtle, it is difficult to decide which solution should be preferred without knowing the probability of the parameter sets.

Table 3 shows the estimates of Cole-Cole parameters obtained deterministically using different sets of initial values. The first one is listed in the last column of Table 2, obtained after several tries by observing the SIP data fits without knowing the true values; the second one uses the true values of the synthetic model. Figure 2 shows the fits to synthetic SIP data with 1% relative noise using the deterministic approach with these two sets of initial values, along with the fit obtained from the stochastic method.

If we did not know the true model parameters, given 1% relative noise in the data, we might be satisfied with the estimates obtained from the first set of initial values. However, comparison with the true Cole-Cole parameters shows that the results in column 4 of Table 3, having the root mean square (rms) of errors of 0.57, is clearly worse than the results in column 3 of the same table, having the rms of 0.084 and obtained from the stochastic inversion method. The estimates found from the second set of initial values (column 5 in Table 3) are best (rms $=$ 0.065) and represent the global solution of the inverse problem because we started from the true Cole-Cole parameters. These estimates are comparable with those (column 3 in Table 3) obtained from the stochastic inversion method.

In practice, we rarely have enough a priori information about SIP mechanisms to choose good initial values that are close enough to the true values to lead to a global optimal solution using the deterministic approach. However, we might desire a single parameter estimate rather than a pdf. We can achieve this goal by using a combination of the stochastic and deterministic approaches, whereby we initialize the deterministic method using the medians of the stochastically obtained marginal posterior pdfs. The sixth column of Table 3 illustrates this approach, and indicates that the obtained estimates are indeed very close (rms $=$ 0.072) to the true Cole-Cole parameters, which are just slightly worse than the results obtained by starting from the true values (rms $=$ 0.065).

Estimated uncertainty information

The stochastic method can provide the entire estimated posterior pdfs and hence extensive information of the unknown parameters. To compare the stochastic estimation results with those obtained using the deterministic method, we use only the 95% highest probability domains (HPDs) of unknown parameters as a measure of uncertainty, which is equivalent to the 95% confidence intervals (CIs) in the deterministic inversion method. Table 4 shows the 95% HPDs of Cole-Cole parameters obtained from the stochastic method and the 95% CIs of estimated parameters from the deterministic inversion method. Note that the upper bound of the possible c_2 range also was set to 1 in the deterministic approach. This table suggests that the stochastic method provides very high precision for all unknown variables; all true values are within the 95% HPDs.

The quality of uncertainty information obtained from the deterministic method varies, depending on the obtained optimal solutions. For initial values given in the last column of Table 2, the resultant estimates do not represent a global solution, as shown in Table 3 and Figure 3. Their 95% CIs are very wide; some do not include the true values. For example, the deterministically obtained time constant τ_2 and dependence factor c_2 shown in Figure 3 vary significantly from the true value. However, when initial values are well chosen (i.e., close to the true values), the deterministic method provides good uncertainty information. For example, when initial values for the deterministic approach are the true values or medians of the stochastic results, the resultant 95% CIs are comparable to those obtained from the stochastic method (except for the zero-frequency resistivity ρ_0).

The uncertainty information obtained from the stochastic method differs from that obtained from the deterministic method by definition. The uncertainty information of the stochastic method depends on the measurement errors in the data and prior distributions, whereas the uncertainty information of the deterministic method is a function of measurement errors in the data and is related to the obtained solution. If the estimated values are close to the true values, the 95% CIs are tight; otherwise, they are inaccurate, as shown in Table 4. For

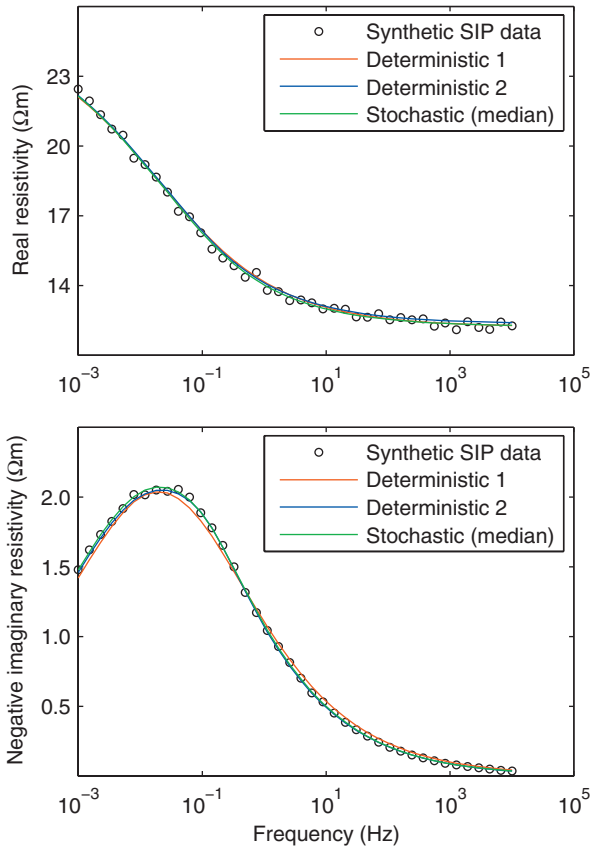

Figure 2. Synthetic SIP data with 1% relative noise and obtained fits using the stochastic method (green curves) and the deterministic method for two sets of initial values (blue curves represent true values, and red curves represent Init0 values in Table 2) for a dual Cole-Cole model.

the stochastic method, as long as the Markov chains converge, we can get good estimates of uncertainty information about the unknown parameters.

LABORATORY STUDIES

Spectral IP laboratory measurements

We use two laboratory SIP data sets measured on unconsolidated sediment samples to compare the performance of the deterministic and stochastic methods for Cole-Cole parameter estimation. The first data set (Figure 4) was measured on a silica-sand sample that had grain size of 125–250 μm and was saturated with a 3×10^{-4} molar KCl solution (Kemna et al., 2005). The data show a Cole-Cole type behavior in the low-to-moderate frequency range (i.e., below 100 Hz) at relatively low polarizability, as is typical of silica sands. Note that the decrease of the real part of resistivity toward lowest frequencies (i.e., below 30 mHz) results from ions being detached from the matrix and going into solution during data acquisition time, which is on the order of two hours for this frequency range. Toward higher frequencies (i.e., above 100 Hz), the data are dominated increasingly by capacitive coupling effects associated with the measurement setup, as is typical in impedance spectroscopy. These coupling effects might be described by the low-frequency branch of a higher-frequency Cole-Cole dispersion term (Kemna et al., 2000).

The second data set (Figure 5) was collected from a sample that was extracted from a sand/gravel aquifer at the Krauthausen test site in Germany (Kemna et al., 2002; Hördt et al., 2007), using the same device and experimental setup used for the first set of laboratory measurements. The sample was saturated with water having an electrical conductivity of approximately 0.05 S/m. The fluvial aquifer at the site partly exhibits a strongly nonuniform grain-size distribution. This is reflected in the selected data set, in which two Cole-Cole type dispersion regions can be identified with phase peaks at approximately 0.1 Hz and 100 Hz, again superimposed by a continuous phase shift increasing toward higher frequencies (i.e., above 1 kHz) as a result of capacitive coupling associated with the measurement layout.

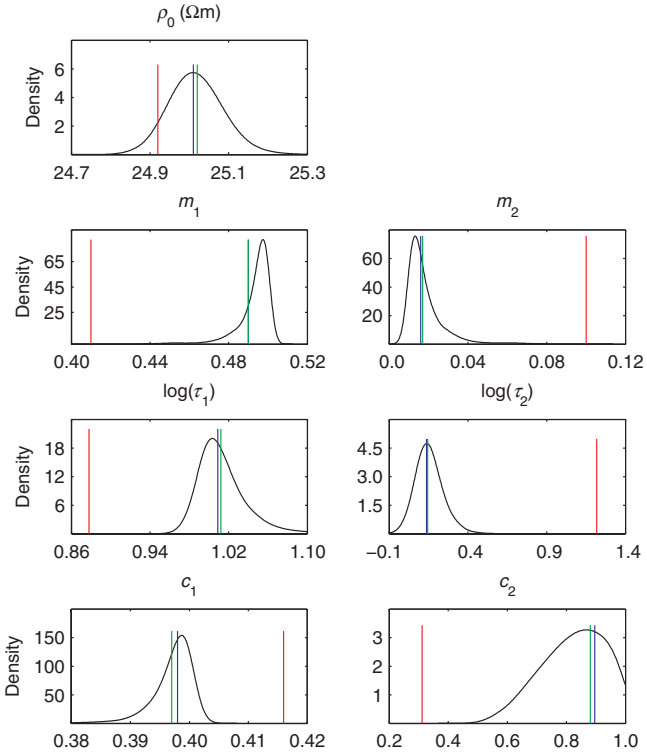

Figure 3. Comparison between estimated pdfs from the stochastic method (black curves) and estimated parameters from the deterministic method for three sets of initial values (blue lines represent true values, green lines represent medians of the stochastic results, and red lines represent estimates using Init0 values in Table 2) for the synthetic SIP data with 1% relative noise using a dual Cole-Cole model.

Inversion of the SIP data from the silica-sand sample

We first inverted the SIP data obtained from the silica-sand sample using the deterministic method for a dual Cole-Cole model. After trying several sets of initial values, we chose the values given in the second column of Table 5. The corresponding estimates of the Cole-Cole parameters and their associated 95% CIs are listed in the third and fourth columns of the same table, respectively. The estimated Cole-Cole parameters seem to fit the SIP data well, as shown by the red curves in Figure 4. For ease of comparison, we calculate the relative half-width (RHW) of 95% CIs by normalizing each actual half-width by the absolute value of its corresponding optimal estimate.

Table 4. Comparison of uncertainty information obtained from inversion of the synthetic SIP data with 1% relative noise using stochastic and deterministic methods.

			Deterministic inversion		
Cole-Cole parameters	True values	Stochastic inversion 95% HPD	95% CI (using Init0)	95% CI (using true values)	95% CI (using medians)
ρ_0 (Ωm)	25.00	(24.89,25.15)	(22.94,26.90)	(23.04,26.97)	(23.05,26.98)
m_1	0.50	(0.475,0.504)	(0,0.869)	(0.484,0.496)	(0.483,0.497)
log(τ_1) (τ_1 in s)	1.00	(0.974,1.066)	(0.538,1.218)	(0.983,1.034)	(0.986,1.038)
c_1	0.40	(0.390,0.402)	(0.352,0.480)	(0.395,0.401)	(0.393,0.401)
m_2	0.01	(0.007,0.037)	(0,0.567)	(0.013,0.019)	(0.014,0.020)
log(τ_2) (τ_2 in s)	0.00	(−0.008,0.337)	(0.049,2.387)	(−0.092,0.366)	(−0.087,0.377)
c_2	0.98	(0.635,1.0)	(0.114,0.508)	(0.738,1.0)	(0.726,1.0)

We can see that the obtained CIs of the estimates overall are tight (RHW $<$ 6%), except for those of m_2 (RHW = 101%), $\log(\tau_1)$ (RHW = 10%), and $\log(\tau_2)$ (RHW = 25%). Note that the lower bound of the possible m_2 range is set to 0.

We also inverted the same SIP data set for a dual model using the stochastic method. We used common prior ranges for the two sets of Cole-Cole model parameters, i.e., (1, 1000) (in Ωm) for zero-frequency resistivity, (−5, 0) ($\log(m)$) for chargeability, (−10, 10) ($\log(\tau)$, τ in seconds) for time constant, and (0, 1) for dependence factor. Following the two-step procedure described in the section of synthetic studies, we obtained the estimated marginal posterior pdfs of the Cole-Cole parameters. For comparison with the deterministic results, we list the medians and their corresponding 95% HPDs in Table 5. Except for chargeability m_2 and time constant $\log(\tau_2)$, which are poorly constrained by the data, the medians of the estimated posterior pdfs of the Cole-Cole parameters are very close to those

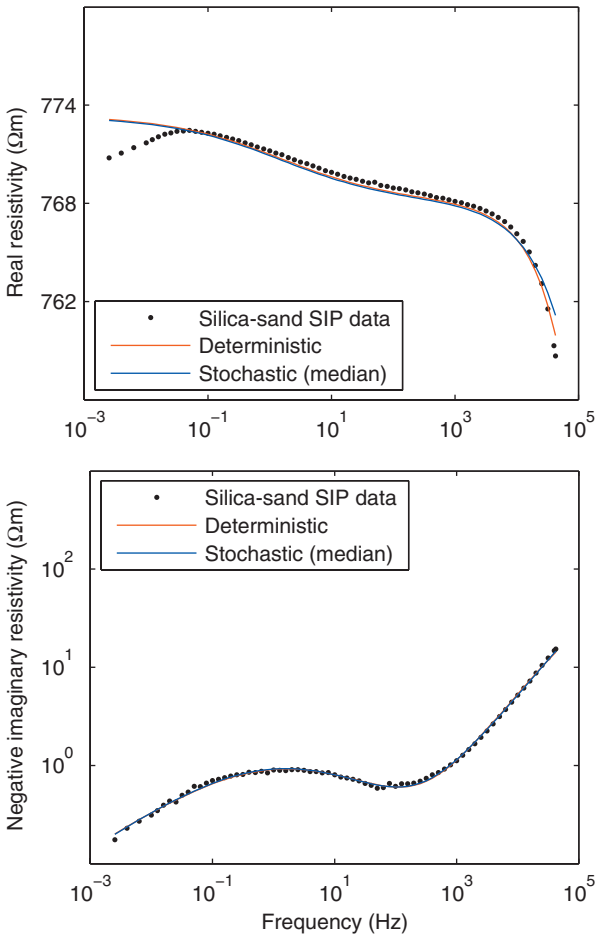

Figure 4. Silica-sand SIP data and fits obtained using the stochastic method (blue curves) and deterministic method (red curves) for a dual Cole-Cole model.

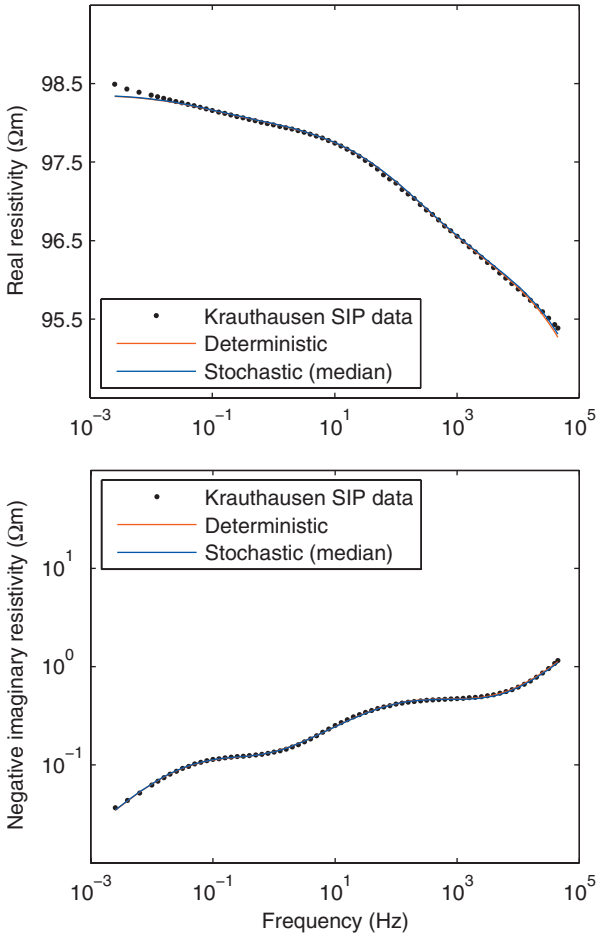

Figure 5. Krauthausen SIP data and fits obtained using the stochastic method (blue curves) and deterministic method (red curves) for a triple Cole-Cole model.

Table 5. Comparison of inversion results using deterministic and stochastic methods for silica-sand SIP data.

	Deterministic method			Stochastic method	
Parameters	Initial values	Estimates	95% CI	Medians	95%HPD
ρ_0 (Ωm)	770.77	773.40	(752.96,794.39)	773.33	(772.38,774.37)
m_1	1e − 3	6.94e − 3	(6.77e − 3,7.11e − 3)	6.90e − 3	(6.7e − 3,7e − 3)
$\log(\tau_1)$ (τ_1 in s)	−1.0	−0.992	(−1.095, −0.889)	−0.972	(−1.005, −0.933)
c_1	0.5	0.418	(0.406,0.429)	0.423	(0.413,0.433)
m_2	1e − 1	1.29e − 1	(0,2.62e − 1)	6.71e − 1	(3.05e − 1,1)
$\log(\tau_2)$ (τ_2 in s)	−6.0	−6.406	(−7.989, −4.823)	−7.462	(−7.734, −6.948)
c_2	1.0	0.765	(0.725,0.804)	0.736	(0.719,0.754)

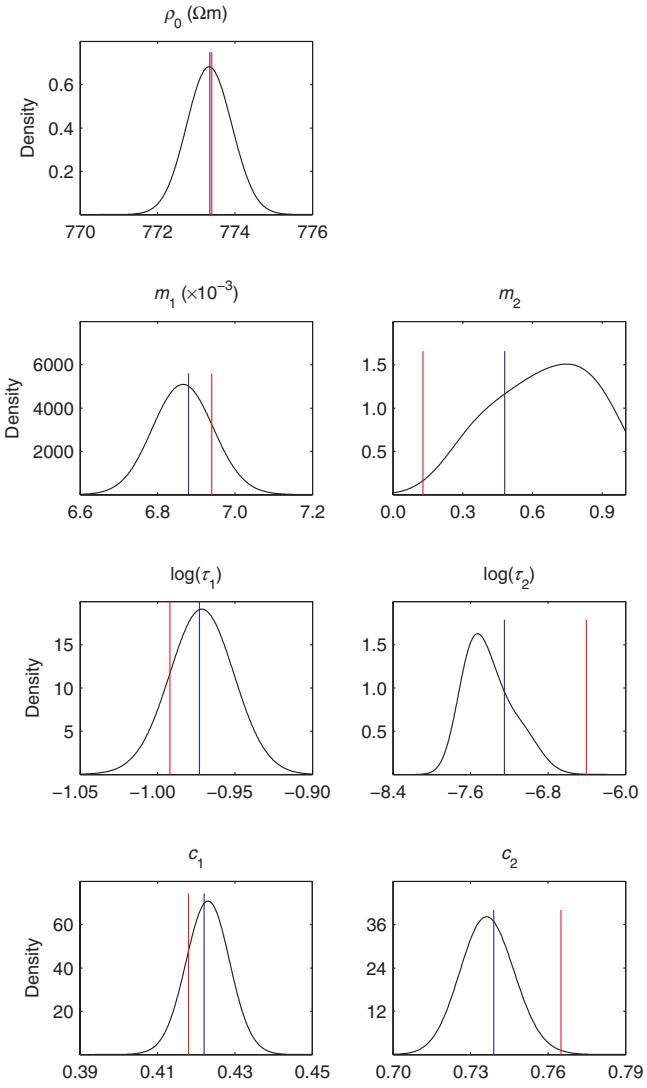

Figure 6. Comparison between estimated pdfs from the stochastic method (black curves) and estimated parameters from the deterministic method for two sets of initial parameters (blue lines represent medians of the stochastic results, and red lines represent values found from test tries) for the silica-sand SIP data using a dual Cole-Cole model.

obtained from the deterministic method. However, the stochastic method provides much tighter uncertainty bounds for those estimates; all relative half-widths of 95% HPDs are less than 3%, except for those of m_2 (RHW = 52%), log(τ_1) (RHW = 4%), and log(τ_2) (RHW = 5%).

Figure 6 compares the estimated pdfs of Cole-Cole parameters obtained from the stochastic method with the optimal estimates obtained from the deterministic method. Except for the time constant log(τ_2) and the dependence factor c_2, all estimates obtained from the deterministic method are within the HPDs of the posterior pdfs. To demonstrate the effect of initial values, we inverted the same data set using the deterministic method starting from the medians of the posterior pdfs. The corresponding new estimates also are shown in Figure 6. Note that all estimated Cole-Cole parameters now are very close to the medians of the estimated marginal posterior pdfs. The new estimates represent a better solution in terms of the chi-square misfit, which is 0.44 for the original initial values and 0.37 for the new initial values.

Table 6 compares the correlation coefficients of Cole-Cole parameters obtained from the deterministic (above slashes) and stochastic (below slashes) methods. These methods give us very small values of crosscorrelation between the zero-frequency resistivity and other parameters. In addition, we can see that the stochastic method provides very similar but slightly smaller values of crosscorrelation among the parameters (m_1, log(τ_1), c_1), which are reasonably constrained by the data, than does the deterministic method. However, the differences in crosscorrelations between parameters involving m_2, log(τ_2), or c_2 are quite large, which might have contributed to the poor resolvability of particularly m_2 and log(τ_2).

Inversion of SIP data from the Krauthausen sand/gravel sample

We also inverted SIP data obtained from the sand and gravel sample from the Krauthausen site using the deterministic and stochastic methods. For the deterministic method, we fitted the data with a triple Cole-Cole model after several tries with different initial values. Table 7 shows the initial values, obtained estimates, and 95% CIs of the estimates. As shown in Figure 5, the estimated Cole-Cole parameters seem to fit the complex resistivity data very well. As in the silica-sand example before, chargeability and time constant of the highest-frequency Cole-Cole terms (i.e., m_3 and log(τ_3)) are not effectively resolved (i.e., exhibit huge 95% CIs; for m_3, the CI actually is given by the preset lower and upper bounds of the allowed range), as expected from the spectral behavior of the data (Figure 5).

Table 6. Comparison of correlation coefficients obtained from deterministic (above slashes) and stochastic (below slashes) methods for silica-sand SIP data.

Parameters	ρ_0	m_1	log(τ_1)	c_1	m_2	log(τ_2)	c_2
ρ_0	1						
m_1	0.01/−0.04	1					
log(τ_1)	0.00/0.01	−0.69/− 0.62	1				
c_1	0.00/−0.02	−0.67/−0.63	0.64/0.60	1			
m_2	−0.01/−0.01	−0.51/−0.12	0.51/0.13	0.39/0.10	1		
log(τ_2)	0.01/0.01	0.52/0.19	−0.52/−0.20	−0.40/−0.16	−0.99/−0.97	1	
c_2	0.01/0.00	0.66/0.59	−0.67/−0.60	−0.53/−0.50	−0.89/−0.33	0.91/0.46	1

Table 7. Comparison of inversion results using deterministic and stochastic methods for Krauthausen SIP data.

	Deterministic method			Stochastic method	
Parameters	Initial values	Estimates	95% CI	Medians	95% HPD
ρ_0 (Ωm)	98.49	98.38	(95.78,101.05)	98.37	(98.25,98.50)
m_1	5e − 3	3.38e − 3	(2.69e − 3,4.07e − 3)	3.4e − 3	(3.2e − 3,3.6e − 3)
$\log(\tau_1)$ (τ_1 in s)	0.0	0.283	(−0.024,0.590)	0.285	(0.239,0.329)
c_1	0.5	0.58	(0.527,0.633)	0.580	(0.562,0.599)
m_2	2e − 2	1.97e − 2	(1.10e − 2,2.83e − 2)	1.97e − 2	(1.82e − 2,2.12e − 2)
$\log(\tau_2)$ (τ_2 in s)	−3.0	−3.13	(−3.876, −2.384)	−3.134	(−3.201, −3.067)
c_2	0.5	0.492	(0.425,0.558)	0.491	(0.474,0.510)
m_3	2e − 1	3.66e − 1	(0,1)	5.318e − 1	(1.753e − 1,9.96e − 1)
$\log(\tau_3)$ (τ_3 in s)	−7.0	−7.998	(−60.318,44.322)	−8.325	(−8.988, −7.263)
c_3	1.0	0.551	(0.425,0.558)	0.551	(0.504,0.604)

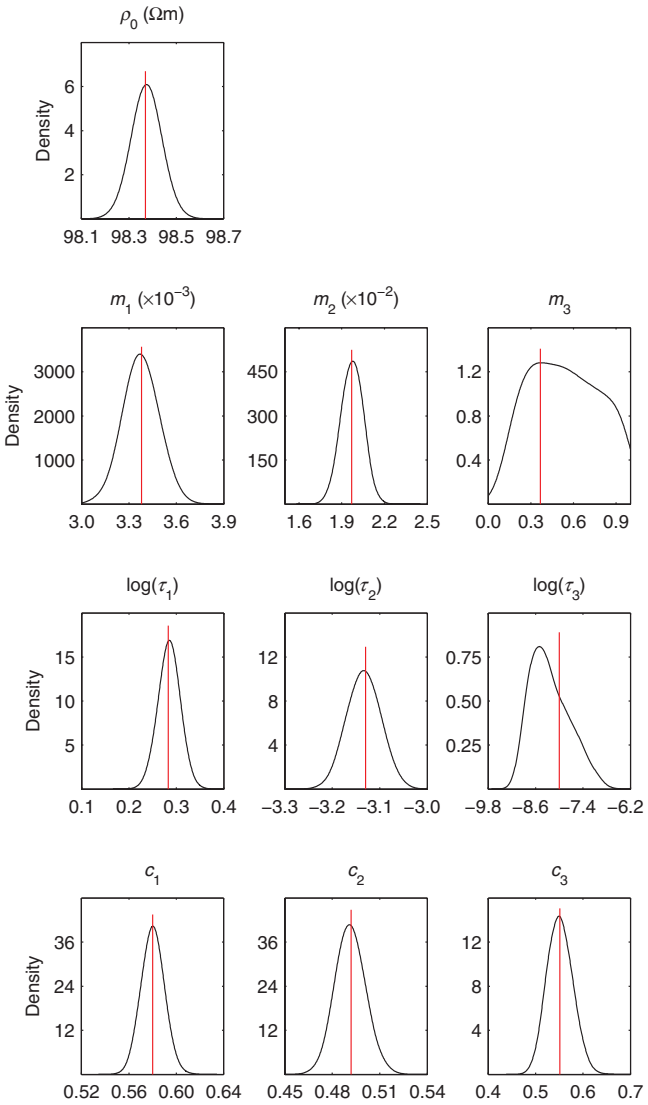

Figure 7. Comparison between estimated pdfs from the stochastic method (black curves) and the estimated parameters from the deterministic method (red lines) for Krauthausen SIP data using a triple Cole-Cole model.

For the stochastic method, we also inverted for the triple Cole-Cole model parameters using common prior ranges. The medians and 95% HPDs of the Cole-Cole parameters are given in the fifth and sixth columns of Table 7. Similar to the silica-sand example, the medians of the estimated pdfs are very close to the optimal solution obtained from the deterministic inversion method, except for m_3 and $\log(\tau_3)$. As shown in Figure 7, all estimates of the Cole-Cole parameters from the deterministic approach are very close to the median of the estimated marginal pdfs. This means that the optimal estimates found by the deterministic method likely represent a global solution for the triple Cole-Cole model. Again, the uncertainty bounds estimated from the deterministic method are much wider than those obtained from the stochastic method, as shown in Table 7. If we assume that the true model indeed is a triple model, the estimated relative errors in real and imaginary components of the SIP data are 0.5% and 1.9%, respectively, which are quite small.

CONCLUSIONS

We developed an MCMC-based Bayesian model to invert for Cole-Cole parameters from SIP data and compared its performance with the commonly used deterministic (Gauss-Newton) method through inversion of synthetic and laboratory data. The Bayesian method estimates marginal posterior pdfs of Cole-Cole parameters using samples obtained from the joint posterior pdf defined by the likelihood functions of SIP data and prior distributions of unknown parameters, whereas the deterministic method seeks the optimal solution by minimizing the squared misfit of the model response with the SIP data. We use noninformative priors in the stochastic method; the estimates of Cole-Cole parameters obtained from the stochastic method primarily depend on the data and thus can be compared to those obtained from the deterministic method. Through detailed comparison between the stochastic and deterministic inversion methods for inverting synthetic and laboratory SIP data, we found that the sampling-based stochastic method has two key advantages over the deterministic method.

The first advantage is that the stochastic method provides a global approach for inverting SIP data for Cole-Cole parameters; the obtained estimates are independent of initial values. The deterministic method is a localized approach for inverting SIP data by finding an optimal solution that fits the SIP data through iteratively updating the model from a starting model of initial values, which typically

must be very close to the true model parameters. Because of the nonlinearity of the forward Cole-Cole modeling and the general nonuniqueness and ill-posed nature of the inverse problem, many local optimal solutions might exist. Consequently, as demonstrated in the synthetic and laboratory data analyses, different initial values can yield different solutions with similar misfit criteria. The MCMC sampling-based stochastic method virtually can start from a wide range of initial values; the obtained Markov chains converge to the target probability distribution. Indeed, it is good to run Markov chains from several very different sets of initial values to detect possible local convergence.

The second advantage is that the stochastic method provides a better way to quantify uncertainty in the inverse problem. The deterministic method estimates the uncertainty of unknown parameters from the diagonal terms of the covariance matrix that is determined by both the regularization and Jacobian matrices evaluated at a presumed optimal solution. The precision of such estimation depends on whether the found minimum is a local or a global minimum and the local characteristics (e.g., nonlinearity and nonuniqueness) of the solution. If the minimum indeed is a local minimum, the estimated uncertainties of the parameters are misleading.

In contrast, the stochastic method estimates the uncertainty of unknown parameters using Monte Carlo approaches. We use MCMC sampling methods to draw many samples of unknown parameters from the joint posterior pdf. As long as those Markov chains converge to the target pdf, the obtained uncertainty information about the unknown parameter is global information, independent of the choice of initial values and the local characteristics of specific solutions.

The MCMC-based inversion method compared to the Gauss-Newton-based inversion methods potentially has two downsides. The first one is that the computation time for the MCMC method is a couple of orders larger than that of the deterministic method. But for IP data inversion, it is not an issue because the running time for the deterministic method is in the order of seconds and that of the stochastic method is in the order of minutes on a PC or laptop, which is acceptable. The second possible limitation of the stochastic method is that it provides marginal probability distribution but not optimal solutions similar to the deterministic method. The users might pick the mean, median, or mode of the marginal probability distribution as the optimal estimate of the unknown parameter. The two methods can complement each other; for example, we can use the stochastic method to find the distribution and use the medians or modes as initial values for the Gauss-Newton method to find one set of optimal solution.

ACKNOWLEDGMENTS

This study was funded by the Department of Energy, Environmental Remediation Science Program (ERSP) grant DE-AC03-76SF00098 to Susan Hubbard. We thank Martin Münch (formerly ICG-4, Forschungszentrum Jülich, Germany) and Odilia Esser (ICG-4, Forschungszentrum Jülich, Germany) who helped with the laboratory SIP measurements included in this study. We also thank the associate editor Dr. John Bradford, Dr. Louise Pellerin, and two anonymous reviewers for their insightful comments and suggestions.

APPENDIX A

DERIVATION OF CONDITIONAL DISTRIBUTION OF THE ZERO-FREQUENCY RESISTIVITY

The derivation of equation 11 is given as

$$
\begin{aligned}
f(\rho_0|\cdot) &\propto \mathrm{Ind}(\rho_0 \in D_\rho) \\
&\quad \times \exp\left\{ -0.5 \sum_{k=1}^{n} \left[u_{\mathrm{Re}} \left(1 - \frac{A(\omega_k)}{\mathrm{Re}[\rho^{obs}(\omega_k)]} \rho_0 \right)^2 \right.\right. \\
&\quad \left.\left. + u_{\mathrm{Im}} \left(1 - \frac{B(\omega_k)}{\mathrm{Im}[\rho^{\mathrm{obs}}(\omega_k)]} \rho_0 \right)^2 \right] \right\} \\
&\propto \mathrm{Ind}(\rho_0 \in D_\rho) \exp\left\{ -0.5 \left[u_{\mathrm{Re}} \sum_{k=1}^{n} \left(\frac{A(\omega_k)}{\mathrm{Re}[\rho^{\mathrm{obs}}(\omega_k)]} \right)^2 \right.\right. \\
&\quad \left.\left. + u_{\mathrm{Im}} \sum_{k=1}^{n} \left(\frac{B(\omega_k)}{\mathrm{Im}[\rho^{\mathrm{obs}}(\omega_k)]} \right)^2 \right] \rho_0^2 \right\} \\
&\quad \times \exp\left\{ \left[u_{\mathrm{Re}} \sum_{k=1}^{n} \left(\frac{A(\omega_k)}{\mathrm{Re}[\rho^{\mathrm{obs}}(\omega_k)]} \right) \right.\right. \\
&\quad \left.\left. + u_{\mathrm{Im}} \sum_{k=1}^{n} \left(\frac{B(\omega_k)}{\mathrm{Im}[\rho^{\mathrm{obs}}(\omega_k)]} \right) \right] \rho_0 \right\} \\
&\propto \mathrm{Ind}(\rho_0 \in D_\rho) \exp\left\{ -\frac{u_\rho^*}{2} (\rho_0 - \mu_\rho^*)^2 \right\} \\
&\propto \mathrm{Ind}(\rho_0 \in D_\rho) N(\mu_\rho^*, u_\rho^*). \qquad \text{(A-1)}
\end{aligned}
$$

APPENDIX B

DERIVATION OF CONDITIONAL DISTRIBUTIONS OF THE INVERSE VARIANCES

The gamma distribution is a conjugate prior for the multivariate normal likelihood function defined in equations 7 and 8; hence posterior distributions of the inverse variances of measurement errors also are gamma distributions as given below,

$$
\begin{aligned}
f(u_{\mathrm{Re}}|\cdot) &\propto f(u_{\mathrm{Re}}) \prod_{k=1}^{n} f(\mathrm{Re}[\rho^{\mathrm{obs}}(\omega_k)]|\rho_0, \mathbf{m}, \mathbf{b}, \mathbf{c}, u_{\mathrm{Re}}) \\
&\propto \{ u_{\mathrm{Re}}^{\alpha-1} \exp(-\lambda u_{\mathrm{Re}}) \} \left\{ u_{\mathrm{Re}}^{0.5n} \exp\left(-0.5 u_{\mathrm{Re}} \right.\right. \\
&\quad \left.\left. \times \sum_{k=1}^{n} \left(\frac{\mathrm{Re}[\rho^{\mathrm{obs}}(\omega_k)] - \mathrm{Re}[\rho(\omega_k)]}{\mathrm{Re}[\rho^{\mathrm{obs}}(\omega_k)]} \right)^2 \right) \right\} \\
&\propto u_{\mathrm{Re}}^{(\alpha+0.5n)-1} \exp\{ -(\lambda + 0.5 S_{\mathrm{Re}}) u_{\mathrm{Re}} \} \\
&\propto \Gamma(\alpha + 0.5n, \lambda + 0.5 S_{\mathrm{Re}}). \qquad \text{(B-1)}
\end{aligned}
$$

Similarly,

$$f(u_{\mathrm{Im}}|\cdot) \propto f(u_{\mathrm{Im}}) \prod_{k=1}^{n} f(\mathrm{Im}[\rho^{\mathrm{obs}}(\omega_k)]|\rho_0, \mathbf{m}, \mathbf{b}, \mathbf{c}, u_{\mathrm{Im}})$$
$$\propto \{u_{\mathrm{Im}}^{\alpha-1} \exp(-\lambda u_{\mathrm{Im}})\} \left\{ u_{\mathrm{Im}}^{0.5n} \exp\left(-0.5 u_{\mathrm{Im}} \times \sum_{k=1}^{n} \left(\frac{\mathrm{Im}[\rho^{\mathrm{obs}}(\omega_k)] - \mathrm{Im}[\rho(\omega_k)]}{\mathrm{Im}[\rho^{\mathrm{obs}}(\omega_k)]} \right)^2 \right) \right\}$$
$$\propto u_{\mathrm{Im}}^{(\alpha+0.5n)-1} \exp\{-(\lambda + 0.5 S_{\mathrm{Im}}) u_{\mathrm{Im}}\}$$
$$\propto \Gamma(\alpha + 0.5n, \lambda + 0.5 S_{\mathrm{Im}}). \quad \text{(B-2)}$$

REFERENCES

Binley, A., L. D. Slater, M. Fukes, and G. Cassiani, 2005, Relationship between spectral induced polarization and hydraulic properties of saturated and unsaturated sandstone: Water Resources Research, **41**, no. 12, W12417.

Boadu, F. K., and B. Seabrook, 2000, Estimating hydraulic conductivity and porosity of soils from spectral electrical response measurements: Journal of Environmental and Engineering Geophysics, **5**, 1–9.

Bosch, M., 1999, Lithologic tomography: From plural geophysical data to lithology estimation: Journal of Geophysical Research, **104**, 749–766.

Buland, A., and H. Omre, 2003, Bayesian linearized AVO inversion: Geophysics, **68**, 185–198.

Cao, Z., Y. Chang, and Y. Luo, 2005, Inversion study of spectral induced polarization based on improved genetic algorithm: Progress in Electromagnetics Research Symposium (PIERS) Online, 1, 266–270; http://piers.mit.edu/piersonline/piers.php; , doi: 10.2529/piers04120094920.

Chen, J., S. Hubbard, J. Peterson, K. Williams, M. Fienen, P. Jardine, and D. Watson, 2006, Development of a joint hydrogeophysical inversion approach and application to a contaminated fractured aquifer: Water Resources Research, **42**, no. 6, W06425.

Chen, J., S. Hubbard, Y. Rubin, C. Murray, E. Roden, and E. Majer, 2004, Geochemical characterization using geophysical data and Markov chain Monte Carlo methods: A case study at the South Oyster Bacterial Transport Site in Virginia: Water Resources Research, **40**, no. 12, W12412.

Cole, K. S., and R. H. Cole, 1941, Dispersion and absorption in dielectrics I: Alternating current field: Journal of Chemical Physics, **1**, 341–351.

Gelman, A., and D. B. Rubin, 1992, Inference from iterative simulation using multiple sequences: Statistical Science, **7**, 457–472.

Geman, S., and D. Geman, 1984, Stochastic relaxation, Gibbs distribution, and Bayesian restoration of images: IEEE Transactions on Pattern Analysis and Machine Intelligence, **6**, 721–741.

Geweke, J., 1992, Evaluating the accuracy of sampling-based approaches to the calculation of posterior moments, J. M. Bernardo, J. O. Berger, A. P. David, and A. F. M. Smith, eds., Bayesian statistics 4: Oxford University Press, 169–193.

Ghorbani, A., C. Camerlynck, N. Florsch, P. Cosenza, and A. Revil, 2007, Bayesian inference of the Cole-Cole parameters from time and frequency domain induced polarization: Geophysical Prospecting, **55**, 589–605.

Gilks, W. R., S. Richardson, and D. J. Spiegelhalter, 1996, Markov chain Monte Carlo in practice: Chapman and Hall.

Gunning, J., and M. E. Glinsky, 2004, Delivery: An open-source model-based Bayesian seismic inversion program: Computers and Geosciences, **30**, 619–636.

Hördt, A., R. Blaschek, A. Kemna, and N. Zisser, 2007, Hydraulic conductivity estimation from induced polarization data at the field scale — The Krauthausen case history: Journal of Applied Geophysics, **62**, 33–46.

Jaggar, S. R., and P. A. Fell, 1988, Forward and inverse Cole-Cole modeling in the analysis of frequency domain electrical impedance data: Exploration Geophysics, **19**, 463–470.

Kemna, A., 2000, Tomographic inversion of complex resistivity: Theory and application: Ph.D. thesis, Ruhr-University Bochum.

Kemna, A., A. Binley, A. Ramirez, and W. Daily, 2000, Complex resistivity tomography for environmental applications: Chemical Engineering Journal, **77**, 11–18.

Kemna, A., H. M. Münch, K. Titov, E. Zimmermann, and H. Vereecken, 2005, Relation of SIP relaxation time of sands to salinity, grain size and hydraulic conductivity: 11th European Meeting of Environmental and Engineering Geophysics, EAGE, Extended Abstracts, P054.

Kemna, A., E. Räkers, and L. Dresen, 1999, Field applications of complex resistivity tomography: 69th Annual International Meeting, SEG, Expanded Abstracts, 331–334.

Kemna, A., J. Vanderborght, B. Kulessa, and H. Vereecken, 2002, Imaging and characterization of subsurface solute transport using electrical resistivity tomography (ERT) and equivalent transport models: Journal of Hydrology, **267**, 125–146.

Leroy, P., A. Revil, A. Kemna, P. Cosenza, and A. Ghorbani, 2008, Complex conductivity of water-saturated packs of glass beads: Journal of Colloid and Interface Science, **321**, 103–117.

Lesmes, D. P., and S. P. Friedman, 2005, Relationships between the electrical and hydrogeological properties of rocks and soils, *in* Y. Rubin and S. Hubbard, eds., Hydrogeophysics: Springer, 87–128.

Luo, Y., and G. Zhang, 1998, Theory and application of spectral induced polarization: SEG, Geophysical Monograph Series, no. 8.

Mansoor, N., and L. Slater, 2007, On the relationship between iron concentration and induced polarization in marsh soils: Geophysics, **72**, no. 1, A1–A5.

Pelton, W. H., W. R. Sill, and B. D. Smith, 1984, Interpretation of complex resistivity and dielectric data: Part II — Geophysical Transactions, **30**, 11–45.

Pelton, W. H., S. H. Ward, P. G. Hallof, W. R. Sill, and P. H. Nelson, 1978, Mineral discrimination and removal of inductive coupling with multifrequency IP: Geophysics, **43**, 588–609.

Raftery, A. E., and S. Lewis, 1992, How many iterations in the Gibbs sampler, *in* J. M. Bernardo, J. O. Berger, A. P. David, and A. F. M. Smith, eds., Bayesian statistics 4: Oxford University Press, 763–773.

Roy, I. G., 1999, An efficient nonlinear least squares 1D inversion scheme for resistivity and IP sounding data: Geophysical Prospecting, **47**, 527–550.

Scott, J. B., and R. D. Barker, 2003, Determining pore-throat size in Permo-Triassic sandstones from low-frequency electrical spectroscopy: Geophysical Research Letters, **30**, 1450 , doi: 10.1029/2003GL016951.

Slater, L., 2007, Near surface electrical characterization of hydraulic conductivity: From petrophysical properties to aquifer geometries — A review: Surveys in Geophysics, **28**, 169–197.

Slater, L. D., J. Choi, and Y. Wu, 2005, Electrical properties of iron-sand columns: Implications for induced polarization investigation and performance monitoring of iron-wall barriers: Geophysics, **70**, no. 4, G87–G94.

Slater, L. D., and D. Lesmes, 2002, IP interpretation in environmental investigations: Geophysics, **67**, 77–88.

Slater, L. D., D. Ntarlagiannis, and D. Wishart, 2006, On the relationship between induced polarization and surface area in metal-sand and clay-sand mixtures: Geophysics, **71**, no. 2, A1–A5.

Spiegelhalter, D. J., K. R. Abrams, N. G. Best, W. R. Gilks, and D. Lunn, 1994, Bayesian inference using Gibbs sampling (BUGS): MRC Biostatistics Unit, Cambridge, England, http://www.mrc-bsu.cam.ac.uk/bugs/.

Tarasov, A., and K. Titov, 2007, Relaxation time distribution from time domain induced polarization measurements: Geophysical Journal International, **170**, 31–43.

Titov, K., V. Komarov, V. Tarasov, and A. Levitski, 2002, Theoretical and experimental study of time domain-induced polarization in water-saturated sands: Journal of Applied Geophysics, **50**, 417–433.

Tong, M., L. Li, W. Wang, and Y. Jiang, 2006, Determining capillary-pressure curve, pore-size distribution, and permeability from induced polarization of shaley sand: Geophysics, **71**, no. 3, N33–N40.

Vanhala, H., 1997, Mapping oil-contaminated sand and till with the spectral induced polarization (SIP) method: Geophysical Prospecting, **45**, 303–326.

Xiang, J., N. B. Jones, D. Cheng, and F. S. Schlindwein, 2001, Direct inversion of the apparent complex-resistivity spectrum: Geophysics, **66**, 1399–1404.